Metrol. Meas. Syst., Vol. 25 (2018) No. 1, pp. 223–234.

PAN POLSKA AKADEMIA NAUK

METROLOGY AND MEASUREMENT SYSTEMS

Index 330930, ISSN 0860-8229

www.metrology.pg.gda.pl

M&MS

APPLICATION OF ION CURRENT MEASUREMENT TO IDENTIFICATION OF COMBUSTION PARAMETERS IN A HOMOGENEOUS CHARGE COMPRESSION IGNITION ENGINE

Jacek Hunicz[1)], Przemysław Filipek[1)], Andrzej Sobiesiak[2)]

1) *Lublin University of Technology, Faculty of Mechanical Engineering, Nadbystrzycka 36, 20-618 Lublin, Poland* (✉ *j.hunicz@pollub.pl*, +48 81 538 4175, *p.filipek@pollub.pl*)

2) *University of Windsor, Department of Mechanical, Automotive & Materials Engineering, 2285 Wyandotte St. W. Windsor, Ont. Canada* (*asobies@uwindsor.ca*)

Abstract

This study examines the application of ion current measurements to the identification of heat release parameters inside the combustion chamber of a homogeneous charge compression ignition (HCCI) engine fuelled with gasoline. HCCI combustion was achieved with the use of exhaust gas trapping. Combustion parameters derived from the in-cylinder pressure and ion current measurements were compared and analysed. Ion current measurements were accomplished using the existing spark plug and a dedicated electronic circuit. The experiments were performed at a variable excess air ratio and a variable amount of trapped residuals. The results showed a good correlation between peak values of the ion current and heat release rate, except for the cases where a fuel-rich mixture was burnt. The computed ion current integral over the volume of the combustion chamber showed a good agreement with the heat released in the combustion chamber, however this parameter was found to be affected by the amount of trapped residuals. Combustion timing characteristic values computed using heat release and ion current were found to be correlated, however the relationship was not linear.

Keywords: HCCI, ion current, heat release rate, combustion control.

1. Introduction

Homogeneous charge compression ignition (HCCI) is a novel combustion technique which offers excellent fuel economy and reduced exhaust emissions. Since the combustion process is initiated by an increase in the temperature inside the combustion chamber, combustion starts at multiple locations simultaneously. Given that combustion is governed by the chemical kinetics of hydrocarbons oxidation rather than by thermodynamic processes, heat release is very rapid and results in the creation of a close to ideal Otto cycle. This increases thermal efficiency of the process when compared with spark ignition or diesel engines. Volumetric combustion of the mixture provides a uniform temperature distribution within the cylinder, which – combined with a high fuel dilution – provides low-temperature combustion. Such a combustion process produces extremely low NO_X emissions and smokeless exhaust [1, 2].

Article history: received on Oct. 01, 2017; accepted on Dec. 16, 2017; available online on Mar. 26, 2018, DOI: 10.24425/118171.

To achieve HCCI combustion, engine designs incorporate different compression ratios, intake air preheating as well as the application of unconventional mechanical designs [3]. HCCI combustion can also be achieved by the application of exhaust gas trapping during an exhaust stroke via negative valve overlap (NVO). The NVO technique enables auto-ignition of gasoline and other high octane number fuels at compression ratios typical of spark ignition engines [4–6].

Auto-ignition timing in HCCI combustion is primarily controlled by compression temperature histories. It is also affected by the mixture composition and its reactivity [7–9]. However, it should be noted that the aforementioned parameters cannot be directly and separately controlled in actual engines. Therefore, the successful implementation of such engines will depend on the development of control technologies. The crucial challenges for HCCI engines include the control of combustion timing in variable operating conditions, the expansion of an operating range in the HCCI mode and engine operation under transient conditions [10–12].

The active control of combustion timing requires a feedback signal. There are a number of approaches to identifying combustion parameters. Besides the reference method consisting in measuring the in-cylinder pressure and performing an analysis based on the first law of thermodynamics, other techniques can be applied, such as optical measurements [13] and ion current sensing [14–16].

Ion current sensing is a viable alternative to expensive piezoelectric in-cylinder pressure transducers. Moreover, there is no need to use an additional sensor, as the existing sparkplug can be used for this purpose. The ion current measurement technique was already applied in spark ignition engines to the identification of misfires and knocking combustion [14]. However, during the spark discharge, ion current readings are distorted. The use of this technique for HCCI engines opens new measurement possibilities. For the operation of an engine in the autonomous HCCI mode, the ignition circuit is switched off, thus the spark plug can be exclusively used as a sensor, providing good insight into the combustion process.

The first effort to utilize ion current sensing to control HCCI combustion was made by Strandh et al. [17]. This initial study demonstrated that the ion signal is a good indicator of combustion phasing. The authors noted that a satisfactory signal-to-noise ratio can be achieved solely for rich mixtures, i.e. for low fuel dilution. A continuation of the research by Vressner et al. [18] revealed that the ion current was sensitive to the type of fuel used; higher signal amplitudes were observed for higher octane numbers. Also, the authors installed a couple of spark plugs in different locations and observed that the recorded signals varied within the space of the combustion chamber. Dong et al. [19] performed a computational study to analyse the mechanism of phase variability between heat release and ion current. The authors found that for lower excess air ratios there was a good agreement between the phasing of ion concentration and the heat release rate, whereas for lean mixtures, the ion signal could be delayed due to a decrease in the ion recombination rate. Butt et al. [20] used different fuel additives to improve the ion current signal at lean mixture conditions. Recently, Liu et al. [21] demonstrated the effect of mixture stratification on the ion current. The application of late fuel injection during the compression stroke resulted in an increase in the ion concentration near the spark plug in the examined engine.

The aim of the present study was to identify ion current signal parameters in a gasoline-fuelled HCCI engine where exhaust gas trapping by NVO was used for initiation of combustion. The engine was run at two valve-train settings providing different amounts of trapped residuals, and at variable excess air. The results of ion current and heat release rate traces were compared to verify the usability of the ion current as a feedback signal for estimating combustion parameters.

2. Experimental apparatus

A single-cylinder research engine fuelled with gasoline was used in the study. The variable valve-train was set such as to provide NVO, and the valve lifts were reduced. Fuel was introduced directly into the cylinder via a side-mounted single-stream swirl-type injector. The most important engine parameters are specified in Table 1.

Table 1. Research engine specifications.

Displaced volume	498.5 cm^3
Cylinder diameter	84 mm
Piston stroke	90 mm
Compression ratio	11.7
No of valves	2
Fuel injector	Solenoid actuated swirl-type
Fuel-rail pressure	11 MPa max.

The engine was installed on the engine test bed equipped with a DC motor as an engine brake. The facility was equipped with all necessary measurement and control instrumentation. In-cylinder pressure was measured with a miniature pressure transducer mounted directly in the engine head, and ion current was detected via an in-house measurement circuit. A data recording system of pressure, ion current and other crank angle-based parameters was triggered by an optical crankshaft encoder with an angular resolution of 0.1 crank angle degrees (CAD). The overall main event excess air ratio was measured with a wide-band lambda probe installed in the exhaust runner. Intake air mass flow rate was measured by a thermal flowmeter. Fuel consumption was provided by a fuel balance. The engine was also equipped with a set of pressure and temperature transducers to control the thermodynamic conditions of all media, intake air, exhaust, cooling liquid, lubricating oil, etc. The engine management system was based on in-house PC software connected with a real-time timing module for controlling injection timing and duration as well as spark generation. A schematic of the experimental setup is shown in Fig. 1.

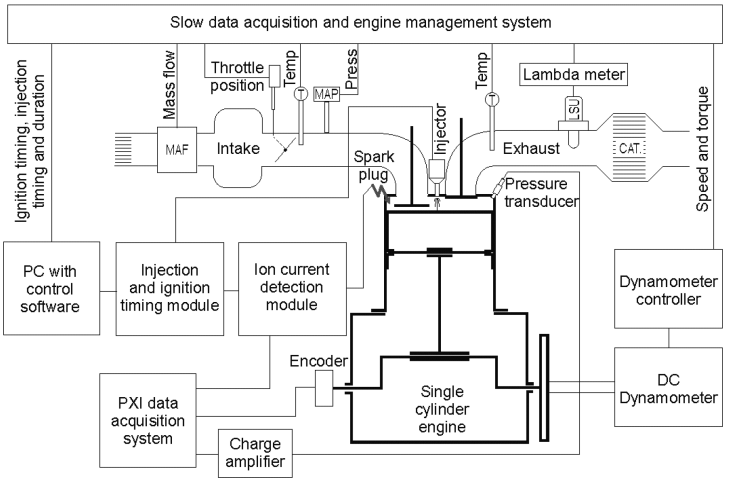

Fig. 1. A schematic of the experimental test stand.

Fig. 2 illustrates the circuit for measuring the ionization current, which consists of an ignition coil, high voltage diodes D_1 and D_2, an external voltage source of 200 V, a current sense resistor R_S and a spark plug. The ion current, proportional to the degree of in-cylinder gas ionization, was measured as a voltage drop on the resistor R_S. The low voltage drop on the resistor R_S was multiplied by a voltage amplifier. The overall sensitivity of the measurement circuit was 0.726 V/μA.

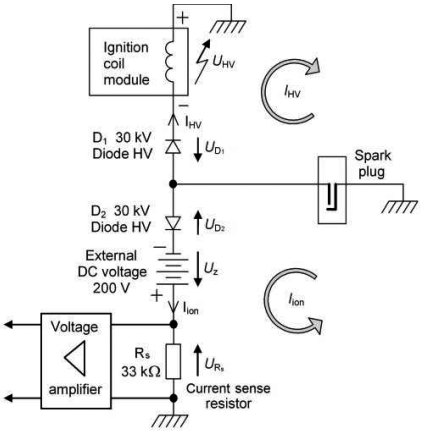

Fig. 2. A schematic of the ion current measurement circuit.

3. Data analysis procedure

Combustion evolution was analysed on the basis of the measured in-cylinder pressure. A heat release rate (HRR) was computed using the first law of thermodynamics in the following form:

$$\mathrm{HRR} = \frac{\gamma}{\gamma-1} p\,dV + \frac{1}{\gamma-1} V\,dp, \tag{1}$$

where V was a volume above the piston, and a ratio of specific heats γ was computed according to instantaneous temperature and mixture composition in the cylinder. However, the HRR refers to the whole combustion chamber. To express a heat release parameter, which can be compared to the locally measured ion current, a power density in the combustion chamber was computed according to the following equation:

$$\mathrm{PD} = \frac{\mathrm{HRR} \cdot \omega}{V}, \tag{2}$$

where ω is an angular speed of the crankshaft. The mass fraction burnt (MFB) of fuel, a measure of how much of the combustion process was completed, was computed as a ratio of the cumulative heat release and the total heat release. The indicated mean effective pressure (IMEP) was utilized to express the combustion system's ability to do work. This measure is independent of the cylinder size and is calculated from the in-cylinder pressure p using the following formula:

$$\mathrm{IMEP} = \frac{1}{V_S} \oint p\,dV, \tag{3}$$

where V_S is a swept volume of the cylinder.

The space-averaged temperature inside the cylinder was computed using the gas equation of state:

$$T = \frac{pV}{mR}, \tag{4}$$

where an in-cylinder mass m included a mass of aspirated air, a mass of trapped residuals and a mass of fuel. Instantaneous values of an individual gas constant R were computed according to the variable mixture composition inside the cylinder. More information on zero-dimensional and one-dimensional engine modelling can be found in [22].

An exhaust gas re-circulation (EGR) rate was expressed as a ratio of the mass of trapped residuals and the entire in-cylinder mass during the main event, including fuel. The fuel dilution ratio was expressed as a ratio of the entire in-cylinder mass and the mass of fuel. An excess air ratio λ was calculated as a ratio of the actual air/fuel ratio and the stoichiometric air demand of fuel on a mass basis.

In the case of the recorded ion current traces, their peak values and locations were referred to heat release parameters. Additionally, to express a quantity representing the amount of energy released during the combustion process, the following ion current integral was determined:

$$I_{ion} = \int_{t_{SOC}}^{t_{EOC}} i_{ion} V \, dt, \tag{5}$$

where t_{SOC} and t_{EOC} are the start and end of combustion time, respectively.

4. Experimental conditions

The experiments were performed at a constant rotational speed of the engine set to 1500 rpm and fully open throttle. The engine was fuelled with European Euro Super commercial gasoline with a research octane number of 95. A fuel sample was analysed according to the ASTM D 5134 standard [23]. The fuel consisted of 38% alkanes, 8% cycloalkanes, 8% alkenes and 37% aromatics. Additionally, the fuel contained 4% ethyl tert-butyl ether and 5% ethanol. The overall carbon-to-hydrogen ratio on a mass basis was 6.43 and the atomic hydrogen-to-carbon ratio was 1.85.

The engine was operated in the NVO mode with the intake valve lift reduced to 3.6 mm and the exhaust valve lift – to 2.9 mm. Two different NVO durations, each defined as an angular gap between the exhaust valve closing and the intake valve opening, were applied: 176 CAD and 163 CAD. Such settings provided fractions of retained residuals in the combustible mixture of approximately 0.55 and 0.4, respectively. An experimental matrix included two excess air sweeps from slightly rich to lean mixture of the engine operating boundary, limited by the occurrence of misfires. The mixture's strength was controlled by the quantity of injected fuel. To achieve the best mixing of fuel and oxidizer, all fuel was injected into the retained residuals, where the start of injection was set to 20 CAD after top dead centre (TDC) of the piston.

Figure 3 shows the engine load expressed by the IMEP and fuel dilution ratio. It should be noted that the effect of λ on IMEP and fuel dilution is much stronger than the one resulting solely from the mixture strength. This is a result of the influence of mixture strength on the amount of trapped residuals. The leaner the mixture and the lower the exhaust temperature are, the higher its density and the mass of trapped residuals become.

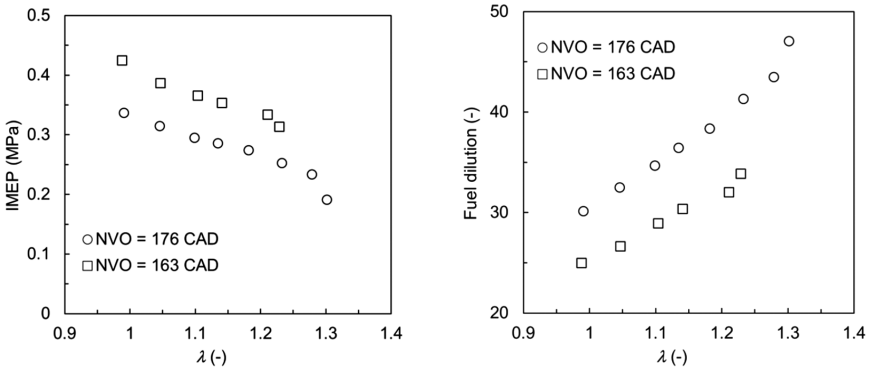

Fig. 3. IMEP (left) and fuel dilution ratio values (right) in respect to the excess air ratio for all investigated conditions.

5. Results and discussion

Fig. 4 shows the ensemble averaged traces of in-cylinder pressure in all investigated conditions. It should be noted that the trends in combustion timings are not monotonic in respect to excess air. For both investigated cases the most advanced start of combustion was observed at a slightly lean mixture ($\lambda \approx 1.05$). The application of both the richer and leaner mixtures resulted in a retard of combustion. More information about combustion evolution is provided by the heat release curves shown in Fig. 5. The peak values of heat release are correlated with combustion timing. The highest values of the peak HRR were observed at $\lambda \approx 1.05$. These trends in combustion timing result from two dominant factors: the excess air itself and the extent of NVO fuel-exhaust reactions. An increase in excess air obviously leads to a higher fuel dilution, which reduces the reaction rates. This effect is additionally enhanced by an accompanying increase in the amount of trapped residuals. The second factor is the effect of excess air on fuel reforming during the NVO period. At lean mixtures, fuel-exhaust reactions produce high amounts of auto-ignition promoting species and, additionally, lead to an increase in compression temperatures due to the thermal effects of partial fuel oxidation [24, 25]. Thus, a reduction of reaction rates at near stoichiometric mixtures can be attributed to reduced NVO exhaust-fuel chemistry, whereas in the range of lean mixtures, an increased fuel dilution is the major factor behind combustion delay.

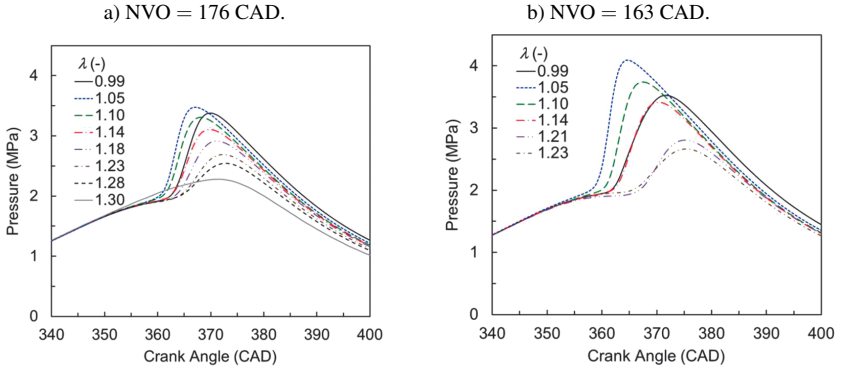

Fig. 4. An in-cylinder pressure in respect to a crank angle.

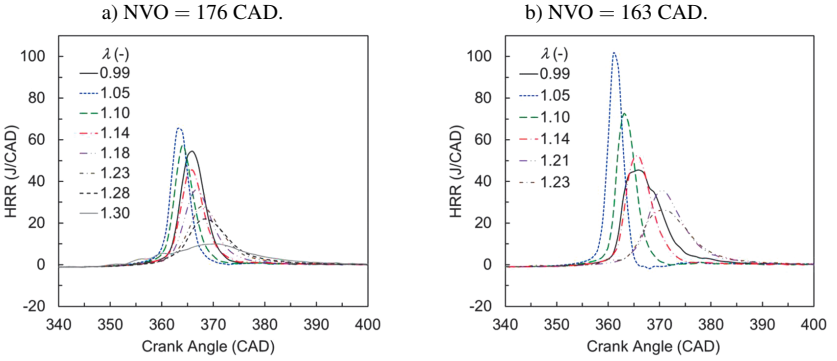

Fig. 5. A computed heat release rate in respect to a crank angle.

The ion current traces shown in Fig. 6 exhibit trends similar to the ones observed for heat release rates. It should be noted, however, that an analysis of the ensemble average values may introduce an aberration resulting from cycle-by-cycle combustion variability. This observation especially refers to the ion current traces with very narrow peaks. For example, for NVO = 163 CAD and $\lambda = 1.14$ the average value of peak ion current was 5.62 μA, whereas its location was 367.4 CAD. The values read from a 100-cycle ensemble average curve are 2.6 μA and 368, respectively. To compensate for averaging errors, the combustion parameters obtained from the HRR and ion current were compared using the estimates computed for each cycle separately and then averaged.

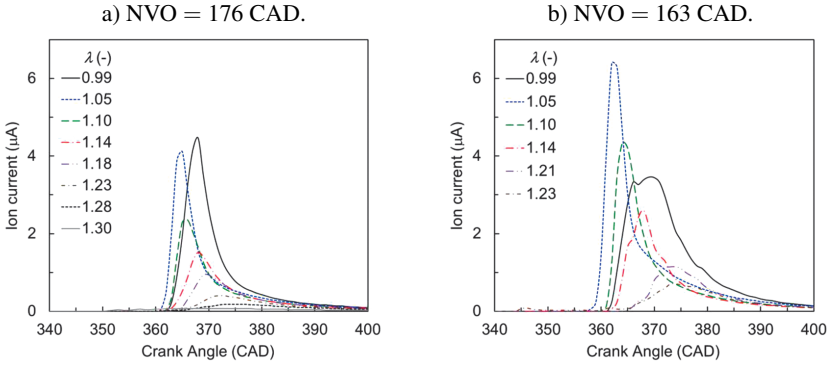

Fig. 6. An ion current in respect to a crank angle.

Fig. 7 shows the correlation between the average peak ion current and the average peak HRR. Additionally, standard deviation (STD) values calculated from 100 consecutive cycles of both quantities are marked by error bars. Overall, there is a good agreement between these two variables, besides rich mixture regime. When the excess air was reduced below the stoichiometric point, the peak ion current further increased while the heat release rates decreased. This observation suggests that the combustion of rich air-fuel mixture reduces reaction rates while at the same time increasing ion concentration. This is plausible because ion concentration is sensitive to temperature, which is obviously determined by mixture strength [26, 27].

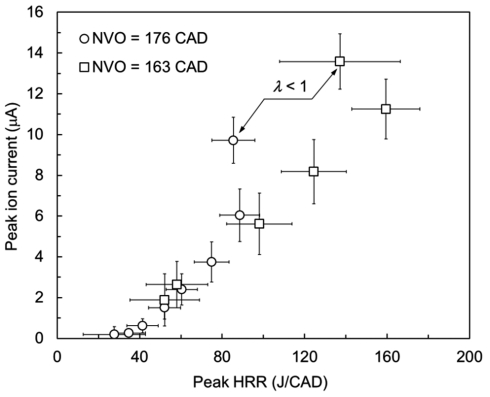

Fig. 7. Peak ion current versus peak HRR. Note depicted data for the rich mixture.

It should be noted that the computed apparent heat release was the average over the whole combustion chamber, whereas the ion current was measured locally, in the area of the spark plug electrodes. To compensate for these effects, the integral of ion current over instantaneous combustion chamber volume was calculated according to (5) and compared with the integral of released heat. The results shown in Fig. 8 (left) indicate that, for each case, all data points follow the same trend. Nevertheless, the trends differ for two investigated NVOs.

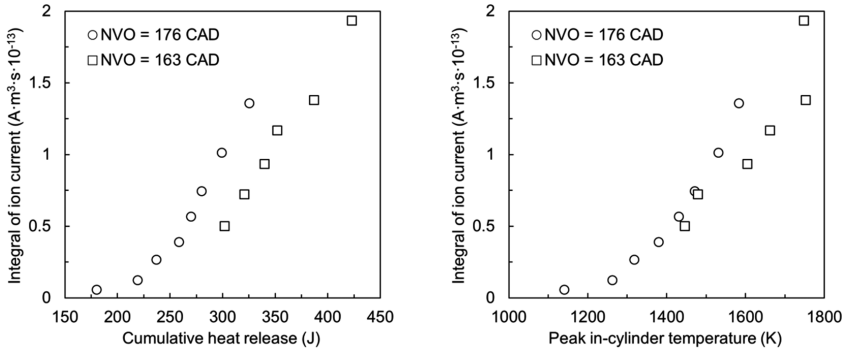

Fig. 8. Integral of ion current versus cumulative heat release (left) and calculated peak in-cylinder temperature (right) for all investigated conditions.

At larger NVO, a higher ion current can be observed, which is plausible because at variable valve timings, the entire in-cylinder mass changes and thus influences the temperature. Fig. 8 (right) shows the correlation between ion current and peak in-cylinder temperature. Obviously, the trend confirms that the concentration of ions is strongly affected by temperature. It can be noted, however, that in a medium temperature range, larger NVO provided a higher ion current, which suggests that the ion current is affected not only by the fuel concentration and temperature, but also by the diluent (i.e. air or residuals causing dilution).

To illustrate the effect of diluent on ion current, Fig. 9 shows the correlation between ion current integral and overall fuel dilution and excess air. The left graph shows that at larger NVO

the observed ion current is higher for a given fuel dilution. In contrast, for a given λ, smaller NVO provides a higher ion current. These trends point to a complex nature of the effects of in-cylinder conditions and mixture composition on the production of ions.

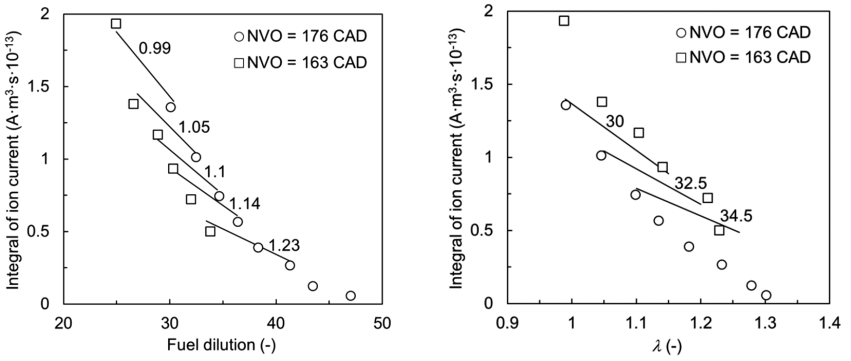

Fig. 9. Integral of ion current versus fuel dilution degree (left) and excess air (right) for all investigated conditions. Lines on graphs connect points of the same λ and dilution accordingly.

The greatest potential of using ion current sensing for the HCCI engine control is the estimation of combustion timing. Fig. 10 shows the correlation between average timings of peak ion current and timings of peak power density calculated according to (2), which could be compared with local measurements of the ion current for a perfectly homogeneous mixture. Additionally, the STD values of both correlated parameters are marked by error bars. The correlation between these parameters shows a good agreement provided that the combustion process occurs early, which is the case with a less diluted mixture. It should be noted that the correlation between the parameters was not affected by the EGR rate. Moreover, the measurement points of rich mixture combustion follow this trend too. In general, the angular location of the peak ion current is delayed when related to the peak power density. However, for leaner mixtures, when approaching the misfire limit, the peak ion current is substantially delayed, whereas the peak power density locations become almost constant. Also, it is worth noticing that there occurs a large variability of combustion timing in this regime.

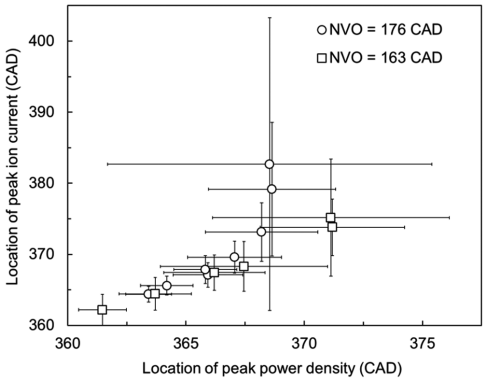

Fig. 10. Location of peak ion current versus location of peak power density.

The trends in ion current timings against the background of characteristic percentages of MFB shown in Fig. 11 demonstrate that the location of peak ion current and MFB depend on fuel dilution. Assuming that around 50% point the MFB traces are linear, in near stoichiometric conditions, the peak ion current correlates with approximately 60% of MFB. However, for higher dilutions, the peak ion current is shifted towards the end of combustion.

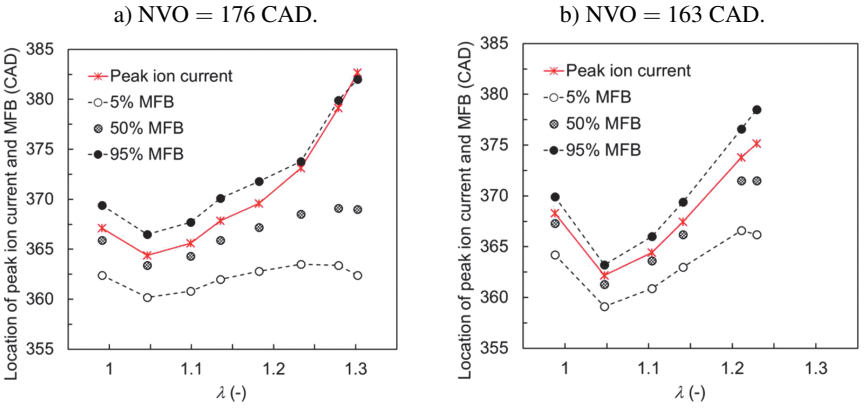

Fig. 11. Location of peak ion current and location of 5%, 50% and 95% MFB versus air excess ratio.

6. Conclusion

Ion current measurements were applied to identify the combustion parameters of residual effected HCCI engine fuelled with gasoline. It was found that the location of peak ion current is well correlated with the location of peak heat release. However, for the lean mixture regime, the ion current was delayed in respect to heat release. An integral of ion current over a volume of the combustion chamber was proposed as an indicator of overall heat release. This quantity showed a good agreement with cumulative heat release. However, it was found to be affected by the amount of internally re-circulated exhaust. An increase in the amount of internally re-circulated exhaust led to a higher ion concentration resulting from the reduction of excess air. It is also plausible that trapped residuals increase the mixture's reactivity as a result of exhaust-fuel reactions during the NVO period.

Acknowledgements

The research was funded by the National Science Centre, Poland under the grant No. 2015/17/B/ST8/03279.

References

[1] Yao, M., Zheng, Z., Liu, H. (2009). Progress and recent trends in homogeneous charge compression ignition (HCCI) engines. *Prog. in Energy Combust. Sci.*, 35, 398–437.

[2] Canakci, M. (2012). Combustion characteristics of a DI-HCCI gasoline engine running at different boost pressures. *Fuel*, 96, 546–555.

[3] Pyszczek, R., Mazuro, P., Teodorczyk, A. (2016). Numerical investigation of CAI Combustion in the Opposed-Piston Engine with Direct and Indirect Water Injection (2016). *IOP Conference Series: Materials Science and Engineering*, 148(1), 012083.

[4] Lavy, J., Dabadie, J.Ch., Angelberger, Ch., Duret, P., *et al.* (2000). Innovative ultra-low NOX controlled auto-ignition combustion process for gasoline engines: the 4-SPACE project. *SAE Technical Paper* 2000-01-1837.

[5] Zhao, H., Li, J., Ma, T., Ladommatos, N. (2002). Performance and analysis of a 4-stroke multi-cylinder gasoline engine with CAI combustion. *SAE Technical Paper* 2002-01-0420.

[6] Yap, D., Karlovsky, J., Megaritis, A., Wyszynski, M.L., Xu, H. (2005). An investigation into propane homogeneous charge compression ignition (HCCI) engine operation with residual gas trapping. *Fuel*, 84, 2372–2379.

[7] Dec, J.E., Yang, Y., Dronniou, N. (2011). Boosted HCCI – controlling pressure-rise rates for performance improvements using partial fuel stratification with conventional gasoline. *SAE Int. J. Engines*, 4, 1169–1189.

[8] Zoldak, P., Sobiesiak, A., Bergin, M., Wickman, D.D. (2014). Computational study of reactivity controlled compression ignition (RCCI) combustion in a heavy-duty diesel engine using natural gas. *SAE Technical Paper* 2014-01-1321.

[9] Mikulski, M., Bekdemir, C. (2017). Understanding the role of low reactivity fuel stratification in a dual fuel RCCI engine – A simulation study. *Appl. Energy*, 191, 689–708.

[10] Lee, M., Oh, S., Sunwoo, M. (2011). Combustion phase detection algorithm for four-cylinder controlled autoignition engines using in-cylinder pressure information. *Int. J. Automot. Technol.*, 12(5), 645–652.

[11] Saxena, S., Bedoya, I.D. (2013). Fundamental phenomena affecting low temperature combustion and HCCI engines, high load limits and strategies for extending these limits. *Prog. Energy Combust. Sci.*, 39, 457–488.

[12] Lee, K., Cho, S., Kim, N, Min, K. (2015). A study on combustion control and operating range expansion of gasoline HCCI. *Energy*, 91, 1038–1048.

[13] Hunicz, J., Piernikarski, D. (2001). Investigation of combustion in a gasoline engine using spectrophotometric methods. *Proc. SPIE Int. Soc. Opt. Eng.*, 4516, 307–314.

[14] Asano, M., Kuma, T., Kajitani, M., Takeuchi, M. (1998). Development of New Ion Current Combustion Control System. *SAE Technical Paper*, 980162.

[15] Filipek, P. (2013). Estimating air-fuel mixture composition in the fuel injection control process in an SI engine using ionization signal in the combustion chamber. *Eksploatacja i Niezawodnosc – Maintenance and Reliability*, 15, 259–265.

[16] Ogata, K. (2014). Investigation of Robustness Control for Practical Use of Gasoline HCCI Engine – An Investigation of a Detecting Technology of Conditions of HCCI Using an Ion Current Sensor. *SAE Technical Paper*, 2014-01-1279.

[17] Strandh, P., Christensen, M., Bengtsson, J., Johansson, R. et al. (2003). Ion Current Sensing for HCCI Combustion Feedback. *SAE Technical Paper*, 2003-01-3216

[18] Vressner, A., Hultqvist, A., Tunestal, P., Johansson, B. et al. (2005). Fuel Effects on Ion Current in an HCCI Engine. *SAE Technical Paper*, 2005-01-2093.

[19] Dong, G., Li, L., Wu, Z., Zhang, Z., Zhao, D. (2013). Study of the phase-varying mechanisms of ion current signals for combustion phasing in a gasoline HCCI engine. *Fuel*, 113, 209–215.

[20] Butt, R.H., Chen, Y., Mack, J.H., Saxena S., Dibble, R.W., Chen, J.Y. (2015). Improving ion current of sparkplug ion sensors in HCCI combustion using sodium, potassium, and cesium acetates: Experimental and numerical modelling. *Proc. Combust. Inst.*, 35, 3107–3115.

[21] Liu, Y., Li, L., Ye, J., Deng, J., Wu. Z. (2016). Ion current signal and characteristics of ethanol/gasoline dual fuel HCCI combustion. *Fuel*, 166, 42–50.

[22] Hunicz, J. (2014). On cyclic variability in a residual effected HCCI engine with direct gasoline injection during negative valve overlap. *Mathematical Problems in Engineering*, 359230.

[23] ASTM International standard (2013). Standard test method for detailed analysis of petroleum naphthas through n-Nonane by capillary gas chromatography. *ASTM Standard* D 5134.

[24] Hunicz, J., Geca, M.S., Kordos P., Komsta H. (2015) An experimental study on a boosted gasoline HCCI engine under different direct fuel injection strategies. *Exp. Therm. Fluid Sci.*, 62, 151–163.

[25] Hunicz, J. (2016). An experimental study into the chemical effects of direct gasoline injection into retained residuals in a homogeneous charge compression ignition engine). *Int. J. Engine Res.*, 17, 1031–1044.

[26] Bogin, G., Chen, J.Y., Dibble, R.W. (2009). The effects of intake pressure, fuel concentration, and bias voltage on the detection of ions in a Homogeneous Charge Compression Ignition (HCCI) engine. *Proc. Combust. Inst.*, 32, 2877–2884.

[27] Dong, G., Chen, Y., Li, L., Wu, Z., Dibble, R. (2017). A skeletal gasoline flame ionization mechanism for combustion timing prediction on HCCI engines. *Proc. Combust. Inst.*, 36, 3669–3676.